LONG-WAVELENGTH OBSERVATIONS OF JETS FROM POLAR REGIONS OF THE SUN

R. RAMESH
Indian Institute of Astrophysics, Bangalore 560034, India

(Received 2 March 1999; accepted 28 June 1999)

Abstract. We report radio observations of enhanced emission associated with the extreme-ultraviolet (EUV) jets from polar coronal hole regions of the Sun, with the Gauribidanur radioheliograph (GRH). We have estimated the brightness temperature, electron density and mass of the ejected material. These jets were not accompanied by nonthermal radio bursts, particularly Type III events.

1. Introduction

In a recent paper, Wang *et al.* (1998) have reported observations of correlated white-light and EUV jets from polar coronal holes with the Large Angle Spectrometric Coronagraph (LASCO, Brueckner *et al.*, 1995) and Extreme-ultraviolet Imaging Telescope (EIT, Delaboudinière, 1995) on the *Solar and Heliospheric Observatory* (SOHO) during the period April 1997 to February 1998. These jets originate near flaring EUV bright points and they are triggered by magnetic reconnection between newly emerged bipolar magnetic fields and neighbouring unipolar flux. Though these jets are similar in appearance to those discovered earlier in soft X-rays with *Yohkoh* (Shibata *et al.*, 1992), they are mainly confined to the polar coronal holes unlike those which occur predominantly in active regions and flaring soft X-ray bright points (Moses *et al.*, 1997). We searched the *Solar Geophysical Data* (1997a,b) for a possible temporal association between these jets and nonthermal radio burst emission, since such an association would identify the flaring EUV bright points with the flare process. None of the events reported by Wang *et al.* (1998) were accompanied by nonthermal emission, particularly Type III radio bursts, as was reported in the case of soft X-ray jets studied by Kundu *et al.* (1995). In this paper, we present evidence for a close association (both spatial and temporal) between the EUV jets and a region of enhanced emission seen in the radio heliograms obtained with the GRH.

2. Observations

The EUV jets reported were observed with the EIT on 19 April 1997 at 05:24 UT and 21 October 1997 at 05:47 UT (Wang *et al.*, 1998). The corresponding white-light jet was seen in the LASCO C2 coronagraph at 06:30 UT. The details of the

Solar Physics **189:** 85–93, 1999.

TABLE I
Details of EIT/LASCO jets

Date	EUV event (UT)	Position angle ($r \approx 1\ R_\odot$) (deg)	Enters C2 (UT)	Position angle ($r \geq 2\ R_\odot$) (deg)
19 Apr. 1997	05:24	182	06:30	183
21 Oct. 1997	05:47	356	06:30	352

TABLE II
Jet speeds

Date	Time (UT)	$V_{\rm lead}$ (km s^{-1})	$V_{\rm cen}$ (km s^{-1})	$V_{\rm init}$ (km s^{-1})
19 Apr. 1997	05:24–07:35	496 ±124	295	292
21 Oct. 1997	05:34–07:23	560 ±140	299	478

jets are given in Tables I and II. One can clearly notice the jets in the LASCO C2 difference images shown in Figures 1 and 2.

The radio images were obtained with the Gauribidanur radioheliograph (GRH, Ramesh *et al.*, 1998) during the local noon at 06:30 UT. Out of the 27 correlated EIT and LASCO events listed by Wang *et al.* (1998), temporal association with the GRH data was available only for the above two events since the duration of observations with the GRH is limited to the meridian at present. The radio observations were made at the same time when the jets were first seen in the LASCO C2 coronograph. The observing frequencies were 75 MHz on 19 April 1997 and 109 MHz on 21 October 1997. The integration time used was 145 ms. This is well suited for observing any transient events like the Type III radio bursts which last for a few seconds. But in the absence of any burst emission, we average the data offline for an effective integration time of about 5 s to minimize the noise. The Sun was 'quiet' and no transient nonthermal burst activity was reported in the *Solar Geophysical Data* (1997a,b) neither at the time of the main EUV event nor during our observational period. The values of the observed peak 'quiet' Sun brightness temperature (T_b) were 1.83×10^5 K at 75 MHz and 3.93×10^5 K at 109 MHz. On both the observing days, excess emission was detected in the radio heliograms (Figures 3 and 5) at the position angle of the jets mentioned in Table I. In Figures 4 and 6, we have plotted the region of enhanced emission alone to bring it out more clearly against the background 'quiet' Sun. The centroid of the region was located at ≈ 2 R$_\odot$ above the limb. The velocity of the jets listed in Table II

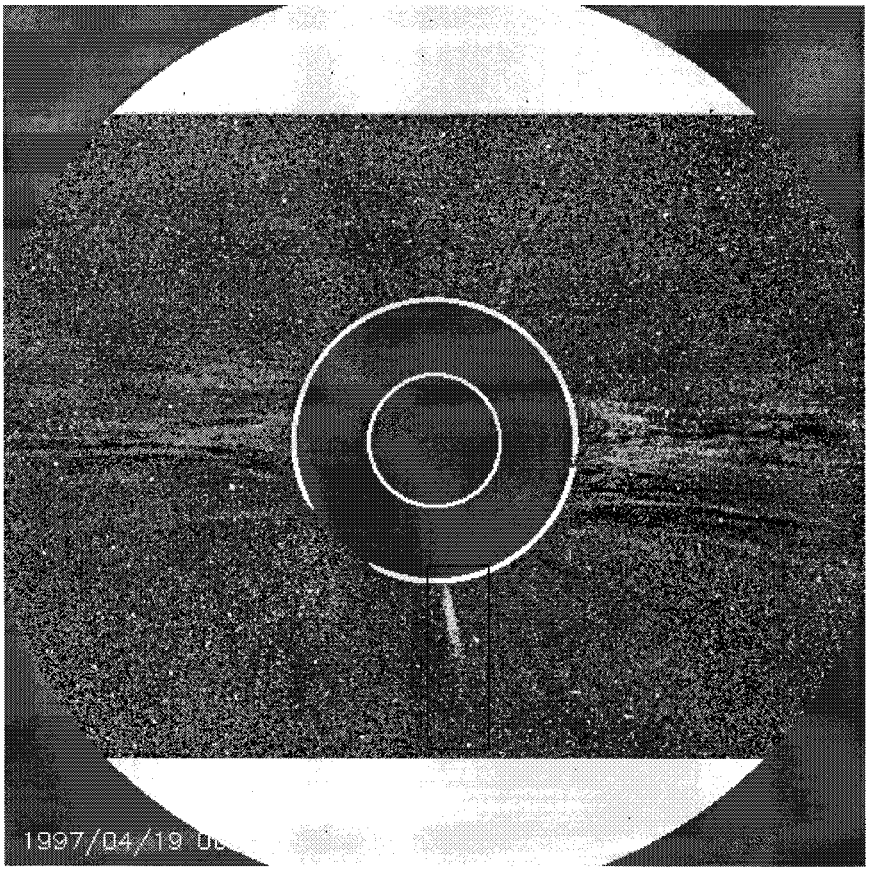

Figure 1. Difference image obtained by subtracting the LASCO C2 image obtained on 19 April 1997 at 05:50 UT from that at 06:30 UT. The field of view is 6.5 $R_\odot$ in the E-W direction and 4.8 $R_\odot$ in the N-S direction. The edge of the outer most of the two circles at the center is at a height of 2.1 $R_\odot$ from the center of the Sun. North is straight up and east is to the left. The location of the jet is indicated by the rectangular box.

indicates that the excess emission was associated with the leading edge of the jet. The brightness temperatures were found to be lower than the corresponding peak value of 'quiet' Sun by about an order of magnitude. Table III gives the details of the region of enhanced emission seen in the GRH maps. One can notice that the values of the various parameters are slightly smaller at 75 MHz compared to 109 MHz in spite of the altitude of the location of the regions being the same at both frequencies. However, it is to be noted that while the time delay between the 75 MHz observations on 19 April 1997 and the main EUV eruption was 66 min, it was only 43 min in the case of 109 MHz observations on 21 October 1997. According to Wang *et al.* (1998), only in a few cases does the material continue to be ejected from the source up to 1 hr after the main EUV event.

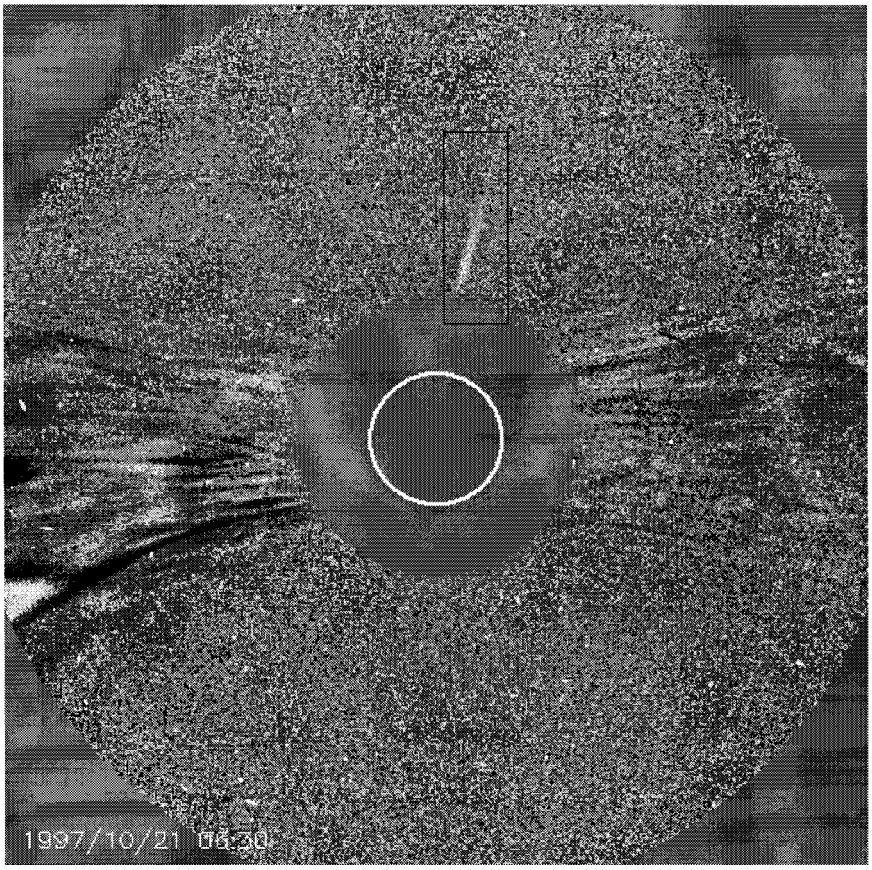

Figure 2. Difference image obtained by subtracting the LASCO C2 image obtained on 21 October 1997 at 06:07 UT from that at 06:30 UT. The field of view is the same as in Figure 1. The location of the jet is indicated by the rectangular box.

TABLE III

Characteristics of the region of enhanced emission seen in the GRH data

Date	Frequency (MHz)	Size (arc min)	T_b (10^4 K)	N_e (10^6 cm^{-3})	Mass (10^{15} g)
19 Apr. 1997	75	28×21	1.27	1.71	4.65
21 Oct. 1997	109	21×19	3.34	4.66	6.43

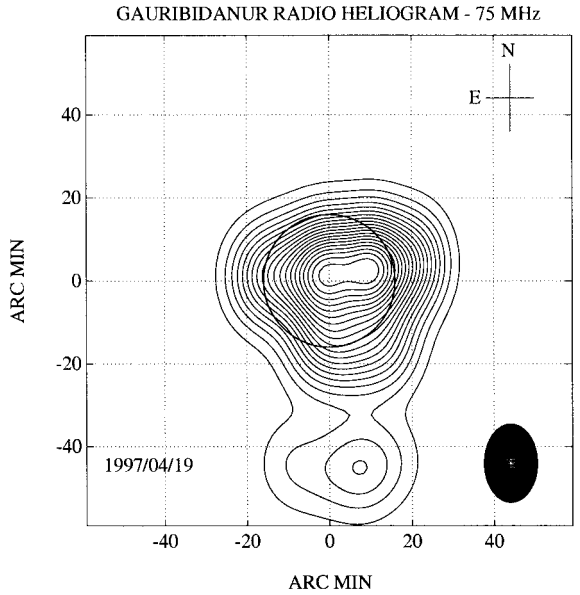

Figure 3. Radio map obtained with the GRH at 06:30 UT on 19 April 1997. The contour levels are from 95 to 5% in steps of 1.83×10^5 K. The open circle at the center is the solar limb. The beam size is indicated by the filled circle at the bottom right-hand corner.

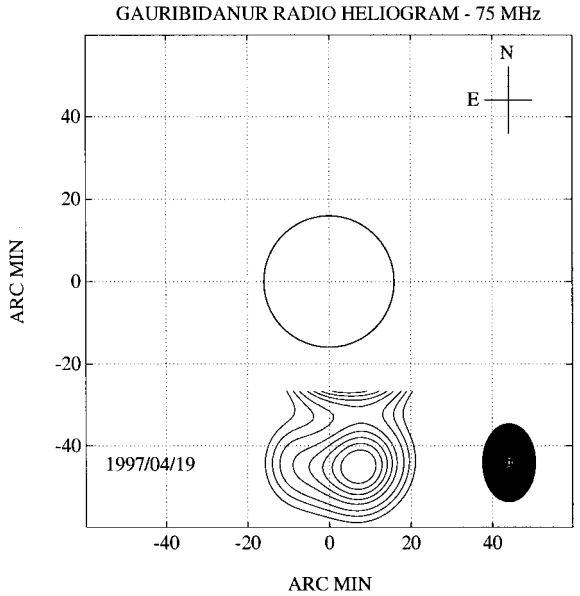

Figure 4. Map of the region of enhanced emission seen in Figure 3. The contour levels are 91, 82, 74, 65, 56, 44, 35, 26% of 1.27×10^4 K.

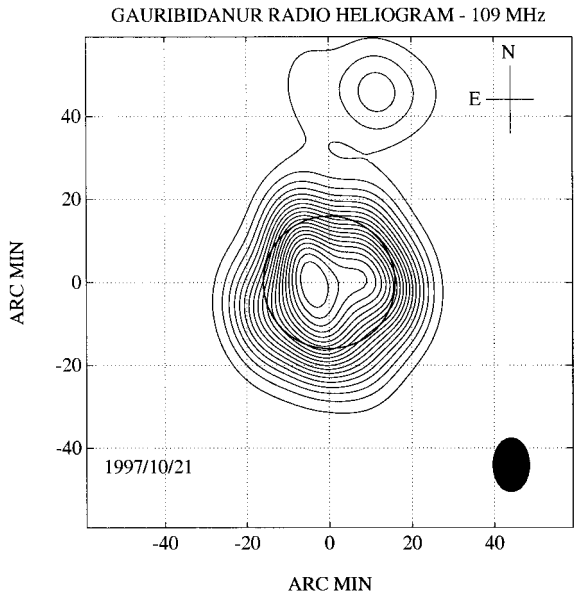

Figure 5. Radio map obtained with the GRH at 06:30 UT on 21 October 1997. The contour levels are from 95 to 5% in steps of 3.93×10^5 K.

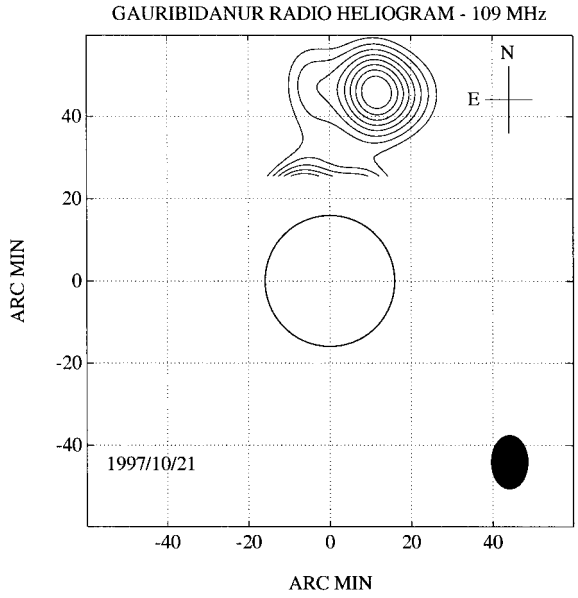

Figure 6. Map of the region of enhanced emission seen in Figure 5. The contour levels are 95, 84, 74, 63, 53, 42, 32% of 3.34×10^4 K.

We would like to point out here that it was possible for us to observe faint features such as those mentioned above mainly because of the calibration scheme that is used for processing of the GRH data. This scheme which effectively makes use of the available redundancy in the length and orientation of the various baseline vectors allows us to image material at brightness temperatures ranging from $\sim 10^4$ K above the background to $\sim 10^6$ K in the same map (Ramesh, 1999).

3. Analysis and Results

Since the electron temperature of the jet is nearly same as the coronal temperature (Wang *et al.*, 1998), it is possible to explain the enhanced radio emission associated with the jets purely on the basis of thermal emission. In order to simulate the observed brightness distribution, we performed ray tracing calculations using Newkirk's density model of the solar corona (Newkirk, 1961). Since the electron density at any point in the corona during the solar minimum is considered to be half of that during the maximum (Thejappa and Kundu, 1994), we have

$$N_e(\rho) = 2.1 \times 10^{4.32/\rho} \left[1 + C_N \exp(-\beta^2/2\,\sigma^2)\right] \mathrm{cm}^{-3}\,, \tag{1}$$

where ρ is the distance from the center of the Sun, β is the distance from the axis of the region of enhanced density and σ is the width of the enhanced region. All distances are in units of the solar radius. The constant C_N determines the density enhancement factor. In the present case, the value of σ was taken to be the same as the lateral width of the discrete source seen in the radio heliogram in Figures 4 and 6. Assuming the background corona to be isothermal with the electron temperature $T_e = 1 \times 10^6$ K, we found from our simulation that for the T_b at a height of approximately 2 $R_\odot$ above the limb to be the same as the observed value, the region of enhanced density should be oriented at an angle of about $\pm 100^\circ$ to the line of sight and the values of C_N should be ≈ 2 and 6 at 75 and 109 MHz, respectively. We were able to account for the increased T_b of the coronal region at the location of the leading edge of the jet by enhancing the density alone and no increase in temperature was required. The orientation of the region of enhanced density in the ray tracing calculation agrees closely with the position angle of the jets mentioned in Table I, as well as the altitude of the region of the enhanced emission in the radio-heliograms.

Since the corona is optically thin far above the limb at frequencies around 80 MHz (Sheridan and Dulk, 1980), one can calculate the electron density using the formula (Sheridan *et al.*, 1978)

$$N_e = \left[5 f^2 T_e^{1/2} T_b L^{-1}\right]^{1/2} \mathrm{cm}^{-3}\,, \tag{2}$$

where f (MHz) is the observing frequency, T_e is the electron temperature, T_b is the observed brightness temperature of the region of enhanced emission and L is the

depth of the region along the line of sight (in units of $R_\odot$). In the present case we assumed the depth to be the same as the observed radial width of the radio source in Figures 4 and 6. Assuming that the coronal plasma is a fully ionized gas of normal solar composition (90% hydrogen and 10% helium by number), one finds that each electron is associated with approximately 2×10^{-24} g of material. Therefore, the mass of the expelled material is given by

$$M = 2 \times 10^{-24} N_e V \text{ g} , \tag{3}$$

where V is the volume of the region of enhanced radio emission. Its value was calculated by multiplying the area of the discrete radio source in Figures 4 and 6 with the assumed depth. The values are 1.36×10^{33} cm^3 and 6.9×10^{32} cm^3 on 19 April 1997 and 21 October 1997, respectively. The kinetic energy of the jets was calculated using the formula $E_{\rm kin} = \frac{1}{2} M V_{\rm lead}^2$, and the values are 5.72×10^{30} ergs and 1.01×10^{31} ergs, respectively, on the above-mentioned two days.

4. Discussion and Conclusions

Simultaneous observations with *Yohkoh* and the Nançay radioheliograph were used by Kundu *et al.* (1995) to show that there is a close spatial and temporal association between the soft X-ray jets in the *Yohkoh* pictures and metric Type III radio bursts. They estimated the value of the electron density at the top of the jet to be $\approx 6.9 \times 10^8$ cm^{-3}. In the present case no Type III radio bursts were observed in spite of the kinetic energy of the jet material being $\sim 10^{31}$ ergs, which is higher than the upper limit of $\sim 10^{29}$ ergs reported for the soft X-ray jets by Shibata (1997). Also, it lies in the range of energy values for the normal flares which is about $10^{29} - 10^{31}$ ergs (Yokoyama and Shibata, 1996). It was shown by Kundu *et al.* (1983) that the Type III emitting nonthermal electrons propagate mainly along dense structures like coronal streamers which have densities ~4–10 times higher than the ambient corona. In spite of an increase in the electron density at the location of the jet, Type III radio bursts were not observed in both events reported here. Since the observations of radio bursts at long wavelengths is a straight forward indicator of the presence of nonthermal population of energetic electrons (Kundu *et al.*, 1994), the lack of their association with EUV bright point flares raises the question regarding the nature of the latter as compared to the normal flares. However, it must be noted that there is not always a one to one correspondence between flares and type III radio bursts. While the statistical association between X-ray flares and type III bursts is 30%, it is only 10% in the case of white-light flares (Dulk, 1985). In spite of these, one cannot rule out the possibility that the bursts are being too weak to be detected by the existing spectrographs in the present case.

Acknowledgements

I express my sincere thanks to Ch. V. Sastry for a critical reading of the manuscript and many valuable suggestions. I thank K. R. Subramanian for his useful comments on the paper, and O. C. St. Cyr for kindly making and supplying the LASCO images. C. Nanje Gowda, G. N. Rajasekara and A.Anwar Saheb are thanked for their help in data collection and maintaining the antenna and receiver system. The SOHO/LASCO data used here are produced by a consortium of the Naval Research Laboratory (USA), Max-Planck-Institut für Aeronomie (Germany), Laboratoire d'Astronomie (France), and the University of Birmingham (UK). SOHO is a project of international cooperation between ESA and NASA.

References

Brueckner, G. E. *et al.*: 1995, *Solar Phys.* **162**, 357.
Delaboudinière, J. P. *et al.*: 1995, *Solar Phys.* **162**, 291.
Dulk, G. A.: 1985, *Ann. Rev. Astron. Astrophys.* **23**, 169.
Kundu, M. R., Gergely, T. E., Turner, P. J., and Howard, R. A.: 1983, *Astrophys. J.* **269**, L67.
Kundu, M. R. *et al.*: 1994, *Astrophys. J.* **427**, L59.
Kundu, M. R. *et al.*: 1995, *Astrophys. J.* **447**, L135.
Moses, D. *et al.*: 1997, *Solar Phys.* **175**, 571.
Newkirk, G., Jr.: 1961, *Astrophys. J.* **133**, 983.
Ramesh, R.: 1999, Ph.D. thesis, Bangalore University.
Ramesh, R., Subramanian, K. R., SundaraRajan, M. S., and Sastry, Ch. V.: 1998, *Solar Phys.* **181**, 439.
Sheridan, K. V., Jackson, B. V., McLean, D. J., and Dulk, G. A.: 1978, *Proc. Astron. Soc. Australia* **3 (4)**, 249.
Sheridan, K. V. and Dulk, G. A.: 1980, in M. Dryer and E. Tandberg-Hanssen (eds.), *Solar and Interplanetary Dynamics*, *Proc. of the IAU Symposium 91*, p. 37.
Shibata, K.: 1997, in *The Corona and Solar Wind Near Minimum Activity*, Proc. of the Fifth SOHO Workshop, p. 103.
Shibata, K. *et al.*: 1992, *Publ. Astron. Soc. Japan* **44**, L173.
Solar Geophysical Data: 1997a, No. 634, Part I.
Solar Geophysical Data: 1997b, No. 640, Part I.
Thejappa, G. and Kundu, M. R.: 1994, *Solar Phys.* **149**, 31.
Yokoyama, T. and Shibata, K.: 1996, *Publ. Astron. Soc. Japan* **48**, 353.
Wang, Y. M. *et al.*: 1998, *Astrophys. J.* **508**, 899.